TÜBİTAK

Turkish Journal of Physics

http://journals.tubitak.gov.tr/physics/

Research Article

Turk J Phys
(2016) 40: 209 – 218

doi:10.3906/fiz-1510-4

The magnetic properties of a quantum dot in a magnetic field

Ayham SHAER, Mohammad K. ELSAID*, Musa ELHASAN
Department of Physics, Faculty of Science, An-Najah National University, Nablus, West Bank, Palestine

Received: 06.10.2015 • **Accepted/Published Online:** 02.05.2016 • **Final Version:** 01.12.2016

Abstract: We calculate the magnetization and susceptibility of two interacting electrons confined in a quantum dot presented in a magnetic field by solving the Hamiltonian using the exact diagonalization method. We investigate the dependence of the magnetization and susceptibility on temperature, magnetic field, and confining frequency. The singlet-triplet transitions in the ground state of the quantum dot spectra and the corresponding jumps in the magnetization curves are shown. The comparisons show that our results are in very good agreement with reported works.

Key words: Magnetization, susceptibility, exact diagonalization, quantum dot

PACS: 73.21.La, 65.80.-g

1. Introduction

Quantum dots (QDs), or artificial atoms, are a subject of research interest due to their physical properties and great potential device applications such as quantum dot lasers, solar cells, single-electron transistors, and quantum computers [1–5]. The application of a magnetic field perpendicular to the dot plane will introduce an additional structure on the energy levels and correlation effects of the interacting electrons that are confined in a quantum dot.

Different approaches were used to solve the two-electrons QD Hamiltonian, including the effect of an applied magnetic field, to obtain the eigenenergies and eigenstates of the QD system. Wagner et al. [6] studied this interesting QD system and predicted the oscillations between spin-singlet (S) and spin-triplet (T) ground states.

Taut [7] managed to obtain the exact analytical results for the energy spectrum of two interacting electrons through Coulomb potential, confined in a QD, just for particular values of the magnetic field strength. In references [8,9] the authors solved the QD Hamiltonian by variational method and obtained the ground-state energies for various values of magnetic field (ω_c) and confined frequency (ω_0). In addition, they performed exact numerical diagonalization for the helium QD-Hamiltonian and obtained the energy spectra for zero and finite values of magnetic field strength. Kandemir [10,11] found the closed-form solution for this QD Hamiltonian and the corresponding eigenstates for particular values of the magnetic field strength and confinement frequencies. Elsaid [12–16] solved the QD Hamiltonian by the dimensional expansion technique, obtained the energies of the two interacting electrons for any arbitrary ratio of Coulomb to confinement energies, and gave an explanation for the level crossings.

Maksym and Chakraborty [17] used the diagonalization method to obtain the eigenenergies of interacting

*Correspondence: mkelsaid@najah.edu

electrons in a magnetic field and show the transitions in the angular momentum of the ground states. They calculated the heat capacity curve for both interacting and noninteracting confined electrons in the QD presented in a magnetic field. The interacting model showed very different behavior from noninteracting electrons, and the oscillations in these magnetic and thermodynamic quantities like magnetization (M) and heat capacity (C_v) were attributed to the spin singlet-triplet transitions in the ground state spectra of the quantum dot. De Groote et al. [18] also calculated the magnetization, susceptibility, and heat capacity of helium-like confined QDs and obtained the additional structure in magnetization. In a detailed study, Nguyen and Peeters [19] considered the QD in the presence of a single magnetic ion and applied magnetic field taking into account the electron-electron correlation in many-electron quantum dots. They displayed the dependence of these thermal and magnetic quantities, $C_v,\ M,\ and\, \chi$, on the strength of the magnetic field, confinement frequency, magnetic ion position, and temperature. They observed that the cusps in the energy levels show up as peaks in the heat capacity and magnetization. In reference [20], the authors used static fluctuation approximation to study the thermodynamic properties of two-dimensional GaAs/AlGaAs parabolic QDs in a magnetic field.

Boyacioglu and Chatterjee [21] studied the magnetic properties of a single quantum dot confined with a Gaussian potential model. They observed that the magnetization curve showed peaks structure at low temperatures. Helle et al. [22] computed the magnetization of a rectangular QD in a high magnetic field and the results showed the oscillation and smooth behavior in the magnetization curve for both interacting and noninteracting confined electrons.

In an experimental work [23], the magnetization of electrons in a GaAs/AlGaAs semiconductor QD as a function of an applied magnetic field at the low temperature of 0.3 K was measured. Oscillations were observed in the magnetization. To reproduce the experimental results of the magnetization, the authors found that electron-electron interaction should be taken into account in the theoretical model of the QD magnetization.

Furthermore, the density functional theory method was used to investigate the magnetization of a rectangular QD in an applied external magnetic field [24].

Climente et al. [25] studied the effect of Coulomb interaction on the magnetization of quantum dots with one and two interacting electrons.

In this work, we calculated the magnetization and magnetic susceptibility as magnetic quantities for a quantum dot helium atom in which both the magnetic field and the electron-electron interaction were fully taken into account. Since the eigenvalues of the electrons in the QD are the starting point to calculate the physical properties of the QD system, we initially applied the exact diagonalization method to solve the QD Hamiltonian and obtained the eigenenergies. After that we used the computed eigenenergy spectra to theoretically display the behavior of magnetization and magnetic susceptibility of the QD as a function of magnetic field strength, confining frequency and temperature.

The rest of this paper is organized as follows: Section 2 presents the Hamiltonian theory and computation diagonalization technique of the interacting quantum helium atom. In Section 3, we show the calculation of the magnetization and susceptibility from the mean energy expression. We devote the final section to numerical results and conclusions.

2. Theory

In this section we describe in detail the main three parts of the theory, namely the QD Hamiltonian, the exact diagonalization method, and the magnetization and magnetic susceptibility.

2.1. Quantum dot Hamiltonian

The effective mass Hamiltonian for two interacting electrons confined in a QD by a parabolic potential in a uniform magnetic field of strength B, applied along the z direction, is given by:

$$\hat{H} = \sum_{j=1}^{2} \left\{ \frac{1}{2m^*} \left[p\left(r_j\right) + \frac{e}{c} A\left(r_j\right) \right]^2 + \frac{1}{2} m^* \omega_0^2 r_j^2 \right\} + \frac{e^2}{\epsilon \left| r_1 - r_2 \right|}, \tag{1}$$

where ω_0 and ϵ are defined as the confining frequency and the dielectric constant for the GaAs medium, respectively. $r_1 and\, r_2$ describe the positions of the first and second electron in the xy plane. ω_c is the cyclotron frequency and $A = \frac{1}{2} B \times r$ is the vector potential. By expressing the Hamiltonian explicitly in terms of coordinates and momenta, Eq. (1) becomes the following:

$$\hat{H} = \frac{1}{2} m\, {r_1}^2 \omega_o^2 + \frac{1}{2} m\, r_2^2\, \omega_o^2 + \frac{e^2}{\epsilon \left| r_2 - r_1 \right|} + \frac{\left(p_1 + \frac{eA[r_1]}{c} \right)^2}{2m} + \frac{\left(p_2 + \frac{eA[r_2]}{c} \right)^2}{2m}. \tag{2}$$

We decoupled the QD Hamiltonian into center of mass (R) and relative (r) parts using the standard coordinate transformations:

$$R = \frac{r_1 + r_2}{2}, \tag{3}$$

$$r = r_2 - r_1, \tag{4}$$

$$P_R = p_1 + p_2, \tag{5}$$

$$p_r = \frac{p_2 - p_1}{2}, \tag{6}$$

The Hamiltonian takes the following form:

$$\begin{aligned} \hat{H} \;=\; & \frac{\left(\frac{e\, A\left[-\frac{r}{2} + R \right]}{c} p_r + \frac{P_R}{2} \right)^2}{2m} + \frac{\left(\frac{e\, A\left[\frac{r}{2} + R \right]}{c} + p_r + \frac{P_R}{2} \right)^2}{2m} + \frac{1}{2} m \left(-\frac{r}{2} + R \right)^2 \omega_o^2 \\ & + \frac{1}{2} m \left(\frac{r}{2} + R \right)^2 \omega_o^2 + \frac{e^2}{\epsilon r}. \end{aligned} \tag{7}$$

The confining parabolic potential terms are written as:

$$\frac{1}{2} m \left(-\frac{r}{2} + R \right)^2 \omega_o^2 + \frac{1}{2} m \left(\frac{r}{2} + R \right)^2 \omega_o^2 = \frac{1}{4} m r^2 \omega_o^2 + m R^2 \omega_o^2. \tag{8}$$

Using the linear property of the vector potential, we separated the kinetic energy terms into center of mass and relative parts.

$$\frac{\left(\frac{e\, A\left[-\frac{r}{2} + R \right]}{c} p_r + \frac{P_R}{2} \right)^2}{2m} + \frac{\left(\frac{e\, A\left[\frac{r}{2} + R \right]}{c} + p_r + \frac{P_R}{2} \right)^2}{2m} = \frac{\left(\frac{eA[r]}{2c} + p_r \right)^2}{m} + \frac{\left(\frac{2eA[R]}{c} + P_R \right)^2}{4m}. \tag{9}$$

The full QD Hamiltonian in (R, r) coordinates takes the following form:

$$\hat{H} = \frac{\left(\frac{eA[r]}{2c}+p_r\right)^2}{m}+\frac{\left(\frac{2eA[R]}{c}+P_R\right)^2}{4m}+\frac{1}{4}mr^2\omega_o^2+mR^2\omega_o^2+\frac{e^2}{\epsilon r}. \tag{10}$$

Finally, we separated the complete two-electron QD Hamiltonian into center of mass Hamiltonian H_{CM} and relative Hamiltonian part H_r as shown below:

$$H = H_{CM}+H_r, \tag{11}$$

$$H_{CM}=\frac{1}{2M}\left[P_R+\frac{Q}{c}A\left(R\right)\right]^2+\frac{1}{2}M\omega_0^2R^2, \tag{12}$$

$$H_r=\frac{1}{2\mu}\left[p_r+\frac{q}{c}A\left(r\right)\right]^2+\frac{1}{2}\mu\omega_0^2r^2+\frac{e^2}{\epsilon\left|r\right|}, \tag{13}$$

where M is the total mass $= 2m$, Q is the total charge$= 2e$, μ is reduced mass $= \frac{m}{2}$, and q is the reduced charge $= \frac{e}{2}$.

The corresponding energy of this Hamiltonian in Eq. (11) is:

$$E_{total}=E_{CM}+E_r. \tag{14}$$

The center of mass Hamiltonian given by Eq. (12) is a harmonic oscillator type with well-known eigenenergies:

$$E_{CM}=E_{n_{cm},m_{cm}}=\left(2n_{cm}+\left|m_{cm}\right|+1\right)\hbar\sqrt{\frac{\omega_c^2}{4}+\omega_o^2}+m_{cm}\frac{\hbar\omega_c}{2}, \tag{15}$$

where $n_{cm}\, m_{cm}$ are the radial and angular quantum numbers, respectively.

However, the relative motion Hamiltonian part (H_r), given by Eq. (13), does not have an analytical solution for all ranges of ω_0 and ω_c. In this work, we apply the exact diagonalization method to solve the relative part of the Hamiltonian and obtain the corresponding eigenenergies E_r.

2.2. Exact diagonalization method

For the noninteracting case the relative Hamiltonian in Eq. (13) is a single particle problem with eigenstates $|n_r m_r >$ known as Fock–Darwin states [26,27]:

$$|n_r m_r\rangle = N_{n_r m_r}\frac{e^{im_r\phi}}{\sqrt{2\,\pi}}\left(\alpha r\right)^{|m_r|}e^{-\alpha^2r^2/2}L_{n_r}^{|m_r|}\left(\alpha^2r^2\right), \tag{16}$$

where the functions $L_{n_r}^{|m_r|}\left(\alpha^2r^2\right)$ are the standard associated Laguerre polynomials. We calculated the normalization constant $N_{n_r m_r}$ from the normalization condition of the basis, $\langle n_r m_r|n_r m_r\rangle = 1$, which resulted in:

$$N_{n_{rm_r}}=\sqrt{\frac{2n_r!\alpha^2}{\left(n_r+\left|m_r\right|\right)!}}. \tag{17}$$

We used α as a constant, which has the dimensionality of an inverse length.

$$\alpha = \sqrt{\frac{m\omega_o}{h}} \tag{18}$$

The eigenenergies of the QD Hamiltonian given by Eq. (14) consist of the sum of the energies for the center of mass Hamiltonian (E_{cm}) and the eigenenergies (E_r), which are obtained by direct diagonalization to the relative Hamiltonian part. For the interacting case, we applied the exact diagonalization method to solve Eq. (13) and find the corresponding exact eigenenergies for arbitrary values of ω_c and ω_0.

We can write the matrix element of the relative Hamiltonian part using the basis $|n_r m_r>$ as:

$$h_{nn'} = \left\langle n_r, m_r \,|\, \hat{H}_r \,|\, n_r^{'}, m_r \right\rangle = \langle n_r m_r| - \frac{\hbar^2}{2\mu}\,\nabla^2 + \frac{1}{2}\,\mu\,\omega^2 r^2 |\, n_r\, m_r > + \langle n_r m_r \,|\frac{e^2}{\epsilon r}|\, n_r^{|} m_r \,\rangle. \tag{19}$$

The corresponding relative dimensionless energies are:

$$\begin{aligned} E_r/\hbar\omega_0 \;\; &= \;\; h_{nn}/\hbar\omega_0 = [\,(2n+|m_z|+1)\,\sqrt{(1+\frac{\gamma^2}{4})} - \frac{\gamma}{2}\,|m_z|\,]\,\delta_{nn^{|}} \\ &\quad + \frac{\lambda}{\sqrt{2}}\sqrt{\frac{n'!n!}{(n+|m_z|)\,!\;(n+|m_z|)\,!}}\;\times I_{nn'}|m_z|, \end{aligned} \tag{20}$$

where $\gamma = \frac{\omega_c}{\omega_0}$ and $\lambda = \frac{\mathbf{e^2}\alpha}{\hbar\omega_0}$ are dimensionless parameters while $\omega^2 = \omega_0^2 + \frac{\omega_c^2}{4}$ is the effective confining frequency. By changing the coordinate transformation to t-variable by direct substitution to $r = \frac{\sqrt{t}}{\alpha}$ in the integration $I_{nn'} = I_{n_r n_r^{|}}$, we can express the Coulomb energy matrix element in the integral form:

$$< n_r m_r \,|\frac{e^2}{\epsilon r}|\, n_r^{|}\, m_r \;> \propto \; I_{nn'|m_z|} = \int_0^\infty dt\, t\, t^{|m_z|} e^{-t} L_n^{|m_z|}(t)\, L_{n'}^{|m_z|}(t)\, \frac{1}{\sqrt{t}}. \tag{21}$$

We evaluated the above Coulomb energy matrix element in a closed form by using the following Laguerre relation [28]:

$$\int_0^\infty t^{\alpha\,-1}\, e^{-pt} L_m^{\lambda}(at)\, L_n^{\beta}(bt)\, dt \;=$$

$$\frac{\Gamma(\alpha)\,(\lambda+1)_m\,(\beta+1)_n\,p^{-\alpha}}{m!n!} \sum_{j=0}^{m} \frac{(-m)_j\,(\alpha)_j}{(\lambda+1)_j\;j!} \left(\frac{a}{p}\right)^j \sum_{k=0}^{n} \frac{(-n)_k\,(\alpha+j)_k}{(\beta+1)_k\;k!} \left(\frac{b}{p}\right)^k. \tag{22}$$

This closed-form result of the Coulomb energy greatly reduces the computation time needed in the diagonalization process.

In our calculation, we used the basis $|n_r m_r>$ defined by Eq. (16) to diagonalize the relative QD Hamiltonian and obtained its corresponding eigenenergies, E_r

2.3. Magnetization and susceptibility

We evaluated the magnetization of the QD system as the magnetic field derivative of the mean energy of the QD.

$$M\,(T,B,\omega_0) = \frac{-\partial\langle E(T,B,\omega_0)\rangle}{\partial B} \tag{23}$$

The magnetic susceptibility is calculated from M directly as:

$$\chi = \frac{\partial M}{\partial B}, \tag{24}$$

where we computed the statistical average energy as:

$$\langle E(T,B,\omega_0)\rangle = \frac{\sum_{\alpha=1}^{N} E_\alpha e^{-E_\alpha/k_BT}}{\sum_{\alpha=1}^{N} e^{-E_\alpha/k_BT}}. \tag{25}$$

The index α in the sum is taken to be over the energy levels of the QD.

We displayed the dependence of the computed magnetization and susceptibility on the magnetic field ω_c, confining frequency ω_0 and temperature (T).

3. Results and conclusions

We present the results for two interacting electrons in a QD made from GaAs material (effective Rydberg R*$= 5.825\,meV$) in Figures 1–5. Figure 1 shows our computed results for energy, magnetization, and magnetic susceptibility as a function of the strength of the magnetic field for confining frequency $\omega_0 = \frac{2}{3}$ R*. The comparison of the energies with Reference [29] clearly shows excellent agreement.

Figure 1a shows the transition in the angular momentum of the ground state of the QD system as the magnetic field increases. The origin of these transitions is due to the effect of Coulomb interaction energy in the QD Hamiltonian. These transitions in the angular momentum of the QD system correspond to the (S-T) transitions manifesting themselves as cusps in the magnetization curve of the QD. In Figure 1b, we show the dependence of the magnetization on the magnetic field strength for the same fixed values of the confining frequency and temperature. The magnetization shows a peak structure, which is a result of the transition in the angular momentum of the ground state energy as shown and discussed previously. For example, the first peak corresponds to the transition in the angular momentum of the ground state from $m_r = 0$ to $m_r = 1$.

Similar to the magnetization, we display in Figure 1c the behavior of the magnetic susceptibility as a function of the magnetic field strength, and we observed that the magnetic susceptibility has a sharp peak due to the transition of the ground-state angular momentum and that this peak decreases as the magnetic field sweeps.

In all steps of the calculations, convergence is achieved. In Figure 2, we plot the ground state energy against the number of basis (s_p) for $\lambda = 3$. The figure clearly shows the numerical stability of the ground-state energy as the number of the basis increases. For example, the ground-state energies were converged to E_r =4.324, 4.320, 4.319, and 4.319 meV for basis numbers $s_p = 5$, 20, 40, and 50, respectively.

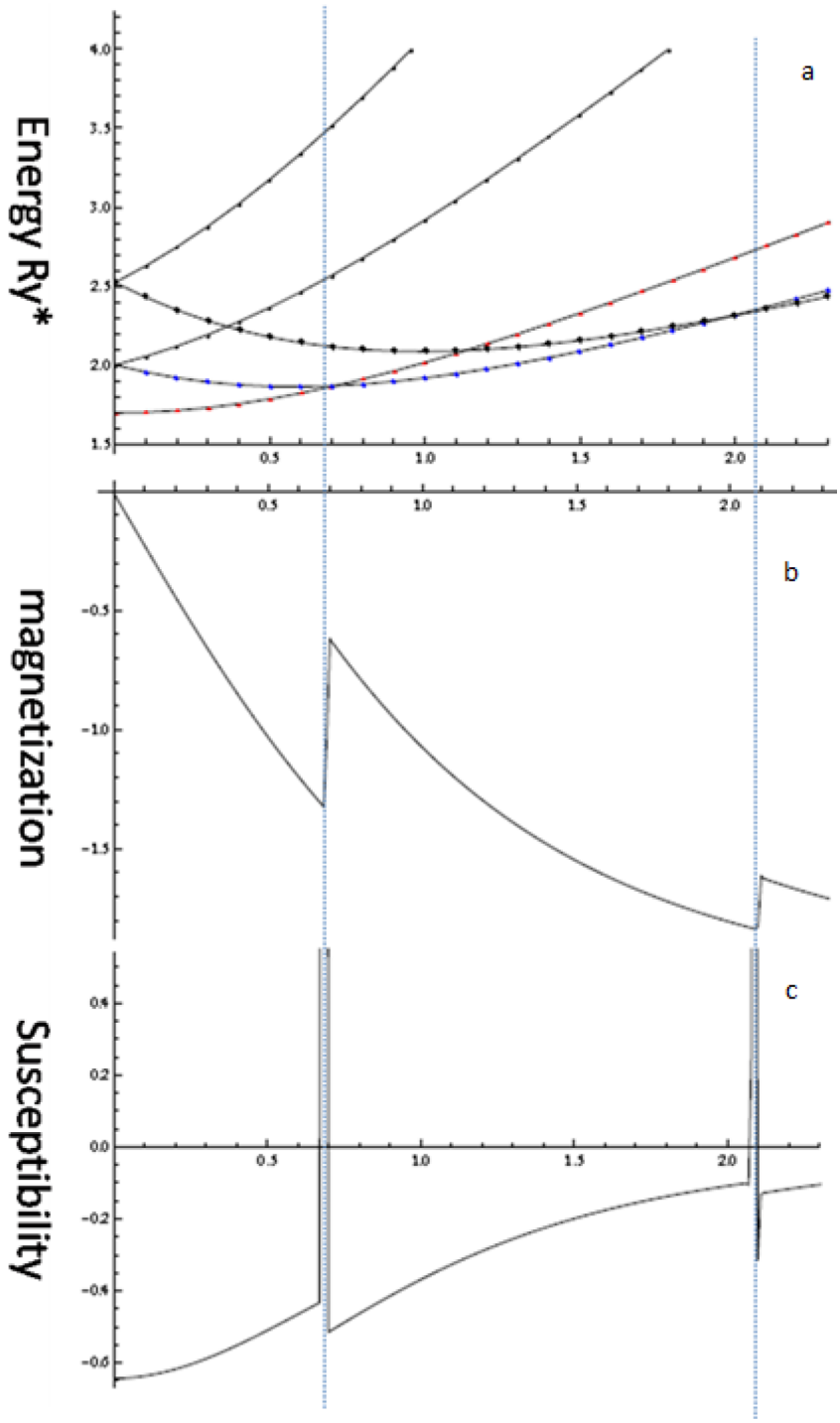

Figure 1. The computed results of two interacting electron QD against the strength of the magnetic field for ω_0=$\frac{2}{3}$ R*. a) The eigenenergy spectra in R*. b) Magnetization (M) in unit of $\mu_B^* = \frac{e\hbar}{2m^*}$ ($\mu_B = 0.87\,meV/T\,for\,GaAs$) at T = 0.01 K. c) Magnetic susceptibility (x) at T = 0.01 K.

To support our magnetization behavior, we plot in Figure 3 the magnetization against the magnetic field for ω_0=$\frac{1}{2}$ and T = 0.01 K, for both interacting and noninteracting electrons in a QD. The noninteracting curve

(solid line) shows a smooth behavior while the interacting curve (dashed line) shows a saw-tooth behavior. The oscillating behavior of the magnetization is caused by Coulomb interaction between the two electrons.

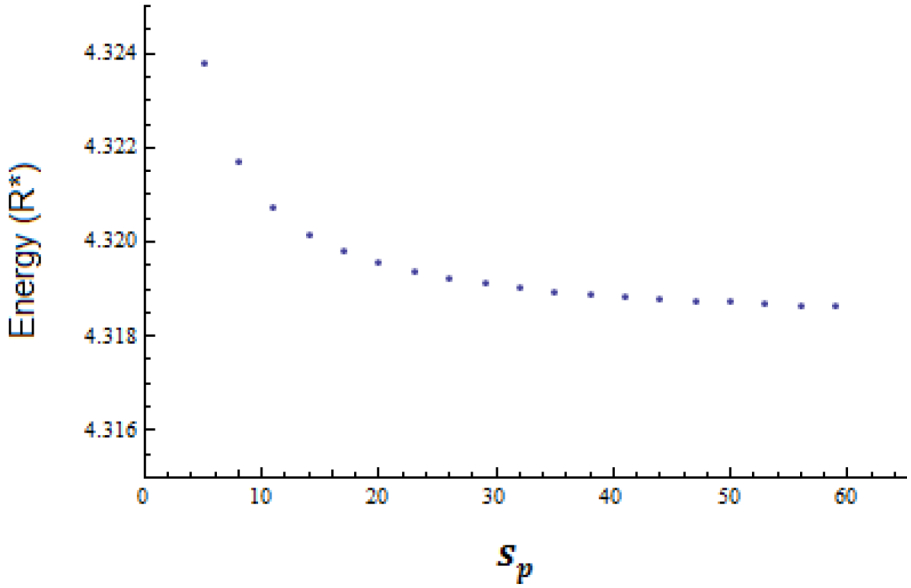

Figure 2. The computed ground state energy of a two-electron QD in zero magnetic field for $\lambda = 3$, where the dimensionless parameter is $\lambda = \frac{e^2\alpha}{\hbar\omega_0}$, against the number of the basis (s_p) taken in the diagonalization process.

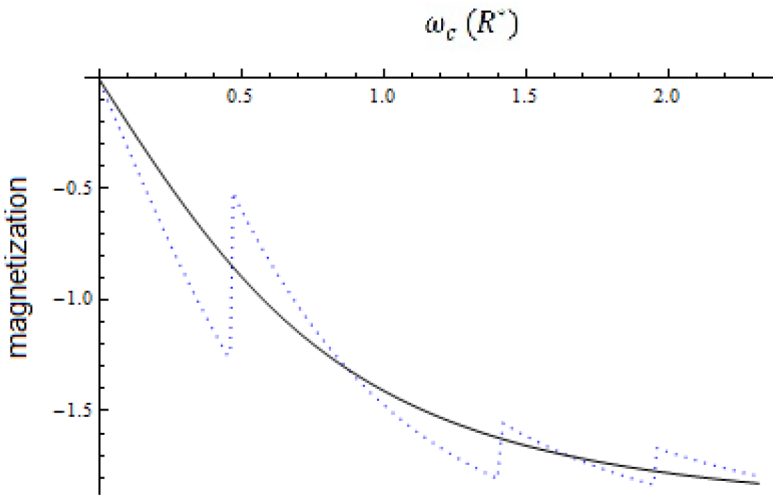

Figure 3. The magnetization (M/μ_B) of two-electron quantum dot for noninteracting (solid line) and interacting (dashed) cases at T = 0.01 K and confinement frequency ($\omega_0 = 0.5$ R*).

In Figure 4, we show the behavior of the magnetization against the magnetic field strength at fixed temperature $T = 0.01\,K$. For various confining frequencies, the peaks in the magnetization curve were shifted to a higher magnetic field as the confining frequency increased. This behavior of the magnetization is in agreement with the results of References [21,25]. In addition, we found that the magnetic susceptibility also had a similar behavior.

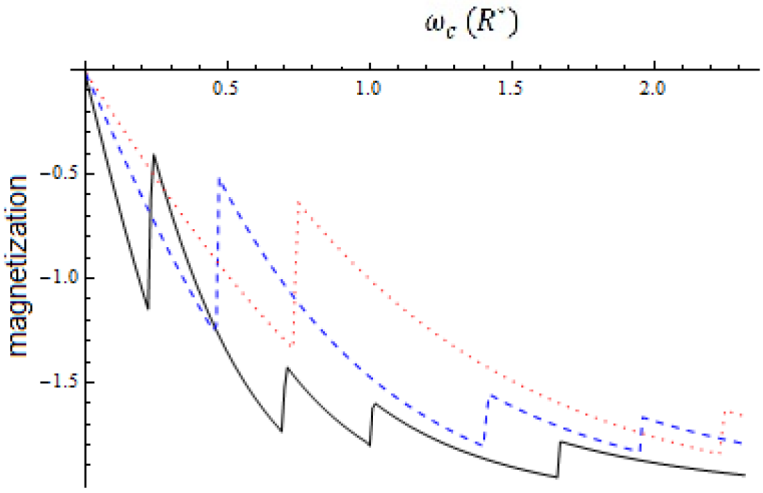

Figure 4. The magnetization (M/μ_B) of two interacting electrons QD as a function of magnetic field strength at T = 0.01 K and various confinement frequencies ω_0 : $\omega_0 = 0.3$, solid; $\omega_0 = 0.5$, dashed, and $\omega_0 = 0.7$, dotted.

In Figure 5, we show the effect of temperature on the magnetization curve for a fixed confining frequency. The curve clearly shows the gradual disappearance of the magnetization jumps as the temperature increases. This behavior is also in agreement with the results of Reference [19]. We also investigated the behavior of the susceptibility and found that the peaks became wider and less sharp.

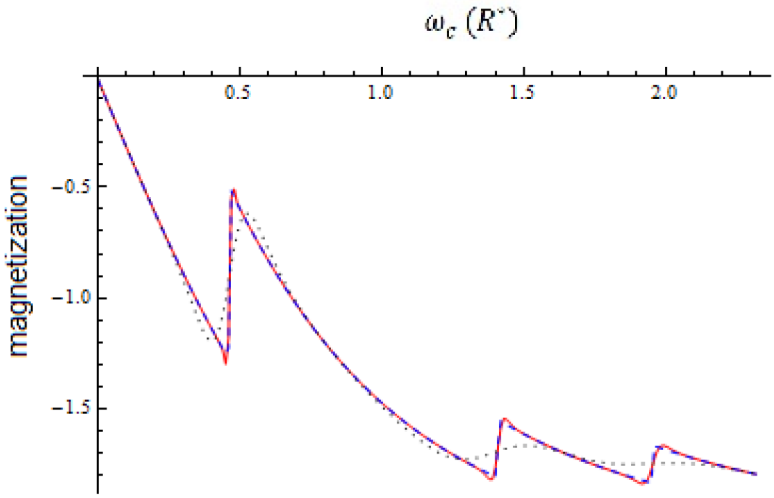

Figure 5. The behavior of the magnetization (M/μ_B) of the two interacting electrons QD as a function of magnetic field strength for fixed value of confining frequency ($\omega_0 = \frac{1}{2}$ R*) and various T: T = 0.01 K, solid; T = 0.1 K, dashed; and T = 1 K, dotted.

In conclusion, the exact diagonalization method was applied as a theoretical approach to solve the Hamiltonian for two interacting electrons that are confined parabolically in a QD presented in a magnetic field. We also studied the dependence of both the magnetization and susceptibility on the magnetic field, confining the frequency and temperature of the system. Moreover, we used the Fock–Darwin states as a basis to evaluate the Coulomb matrix element and to give the result in a closed form. The investigations showed

that the oscillations in magnetization and susceptibility are due to the role of electron-electron interactions, as reported in previous works.

References

[1] Ashoori, R. C.; Stormer, H. L.; Weiner, J. S.; Pfeiffer, L. N.; Baldwin, K. W.; West, K. W. *Phys. Rev. Lett.* **1993**, *71*, 613-616.

[2] Ciftja, C. *Phys. Scripta* **2013**, *72*, 058302.

[3] Kastner, M. A. *Rev. Mod. Phys.* **1992**, *64*, 849-858.

[4] Loss, D.; Divincenzo, D. P. *Phys. Rev. A* **1998**, *57*, 120-126.

[5] Burkard, G.; Loss, D.; Divincenzo, D. P. *Phys. Rev. B* **1999**, *59*, 2070-2078.

[6] Wagner, M.; Merkt, M. U.; Chaplik, A. V. *Phys. Rev. B* **1992**, *45*, 1951-1954.

[7] Taut, M. *J. Phys. A-Math. Gen.* **1994**, *27*, 1045-1055.

[8] Ciftja, C.; Kmar, A. A. *Phys. Rev. B* **2004**, *70*, 205326.

[9] Ciftja, O.; Faruk, M. G. *Phys. Rev. B* **2005**, *72*, 205334.

[10] Kandemir, B. S. *Phys. Rev. B* **2005**, *72*, 165350.

[11] Kandemir, B. S. *J. Math. Phys.* **2005**, *46*, 032110.

[12] Elsaid, M. *Phys. Rev. B* **2000**, *61*, 13026-13031.

[13] Elsaid, M. *Semiconductor Sci. Technol.* **1995**, *10*, 1310-1314.

[14] Elsaid, M. *Superlattice. Microst.* **1998**, *23*, 1237-1243.

[15] Elsaid, M.; Al-Naafa, M. A.; Zugail, S. J. *Comput. Theor. Nanosci.* **2008**, *5*, 677-680.

[16] Elsaid, M. *Turk. J. Phys.* **2002**, *26*, 331-339.

[17] Maksym, P. A.; Chakraborty, T. *Phys. Rev. Lett.* **1990**, *65*, 108-111.

[18] De Groote, J. J. S.; Hornos, J. E. M.; Chaplik, A. V. *Phys. Rev. B* **1992**, *46*, 12773-12776.

[19] Nguyen, N. T. T.; Peeters, F. M. *Phys. Rev. B* **2008**, *78*, 045321.

[20] Nammas, F. S; Sandouqa, A. S; Ghassib, H. B.; Al Sugheir, M. K. *Physica B* **2011**, *406*, 4671-4677.

[21] Boyacioglu, B.; Chatterjee, A. *J. Appl. Phys.* **2012**, *112*, 083514.

[22] Helle, M.; Harju, A.; Nieminen, R. M. *Phys. Rev. B* **2005**, *72*, 205329.

[23] Schwarz, M. P.; Grundler, D.; Wilde, M.; Heyn, C.; Heitmann, D. *J. Appl. Phys.* **2002**, *91*, 6875-6877.

[24] Räsänen, E.; Saarikoski, H.; Stavrou, V. N.; Harju, A.; Puska, M. J.; Nieminen, R. M. *Phys. Rev. B* **2003**, *67*, 235307.

[25] Climente, J. I.; Planelles, J.; Movilla, J. L. *Phys Rev. B* **2004**, 70, 081301.

[26] Fock, V. *Z. Phys.* **1928**, *47*, 446-450.

[27] Darwin, C. G. *Math. Proc. Cambridge* **1930**, *27*, 86-90.

[28] Nguyen, N. T. T.; Das Sarma, S. *Phys. Rev. B* **2011**, *83*, 235322.

[29] Dybalski, W.; Hawrylak, P. *Phys. Rev. B* **2005**, *72*, 205432.